Simulating the Image Chain of the ExoMars 2020 Rover PanCam Wide Angle Cameras

DEPARTMENT OF SPACE & CLIMATE PHYSICS
MULLARD SPACE SCIENCE LABORATORY

Roger B. Stabbins (roger.stabbins.10@ucl.ac.uk) [1,2],
A. D. Griffiths[1,2], A. J. Coates[1,2], M. Gunn[3], C. Huntly[3], F. Trauthan[4], N. Schmitz[4] and the PanCam Science Team

PanCam on the ExoMars 2020 Rover

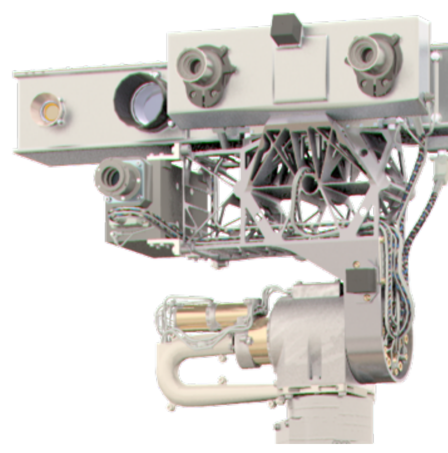

Figure 1: CAD Model of PanCam, also hosting NavCam and ISEM. Credit: ESA

PanCam[1] is a 3 camera system for the ExoMars rover[2], featuring a pair of Wide Angle Cameras (WACs), for 3D stereo vision and multispectral imaging[3], and a High Resolution Camera (HRC), for close-up colour imaging.

The Wide Angles Cameras (WACs)

Optics
38.3×38.3 FOV (°)
11 filters per camera
f# 10.0

Detector
Star 1000 Radiation Hard
Monochrome Sensor
CMOS APS 3T
1024x1024 pixels
15µm Pitch
10-bit ADC

Filters
6 RGB Broadband (3 per WAC)
4 Solar Narrowband (2 per WAC)
12 Geology Narrowband (6 per WAC)

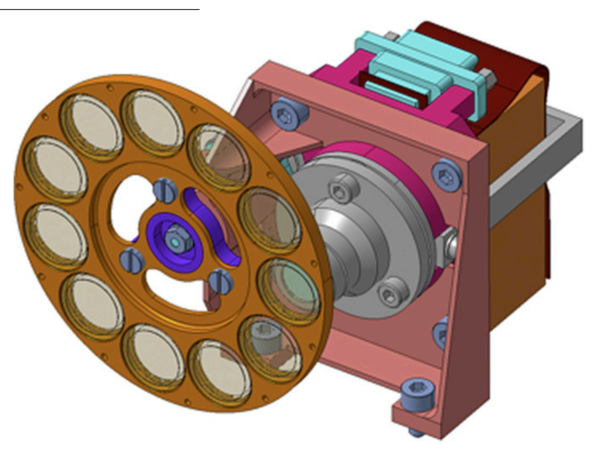

Figure 2: WAC assembly CAD Model, illustrating the filter wheel and camera module. Credit: MSSL

The Image Chain

Information (e.g. 3D structure, mineral presence, grain size etc), can be inferred from an image by formulating and solving an inverse problem, g. The type of inverse problem used is dependent on the form of the forward problem, f, and in particular the distribution of noise.[3]

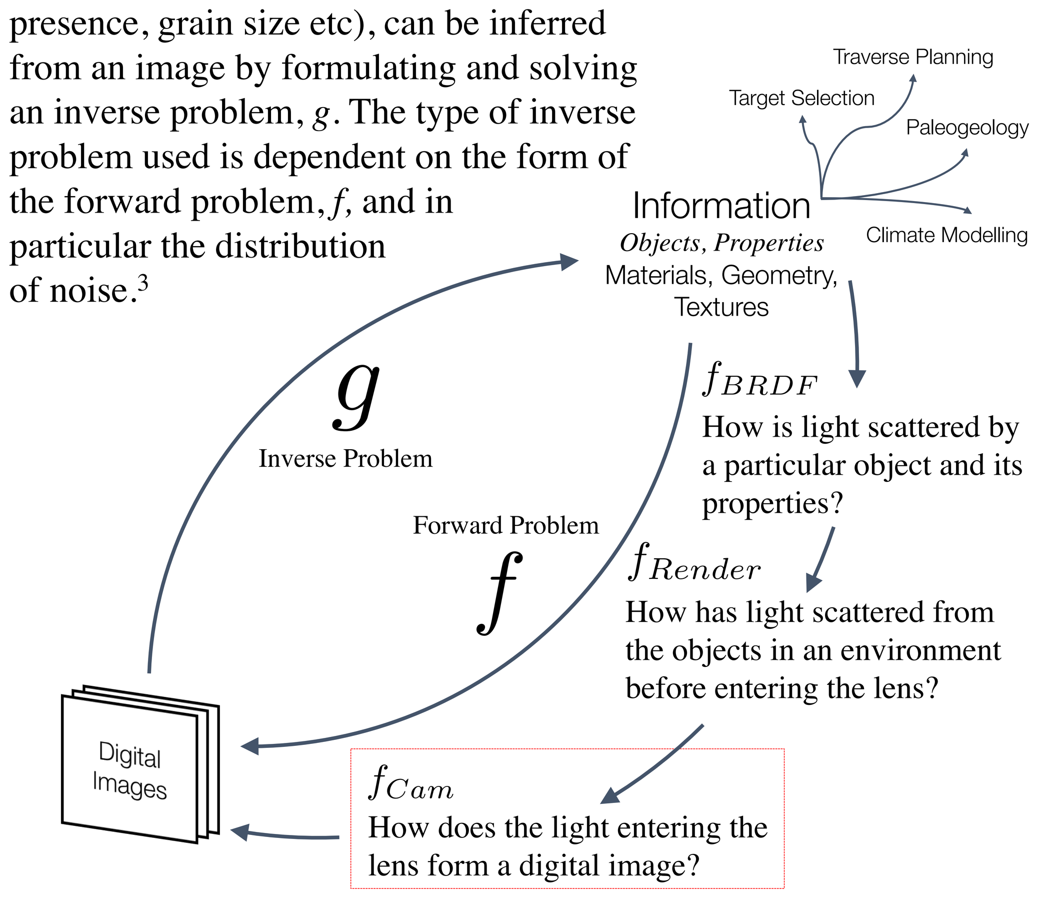

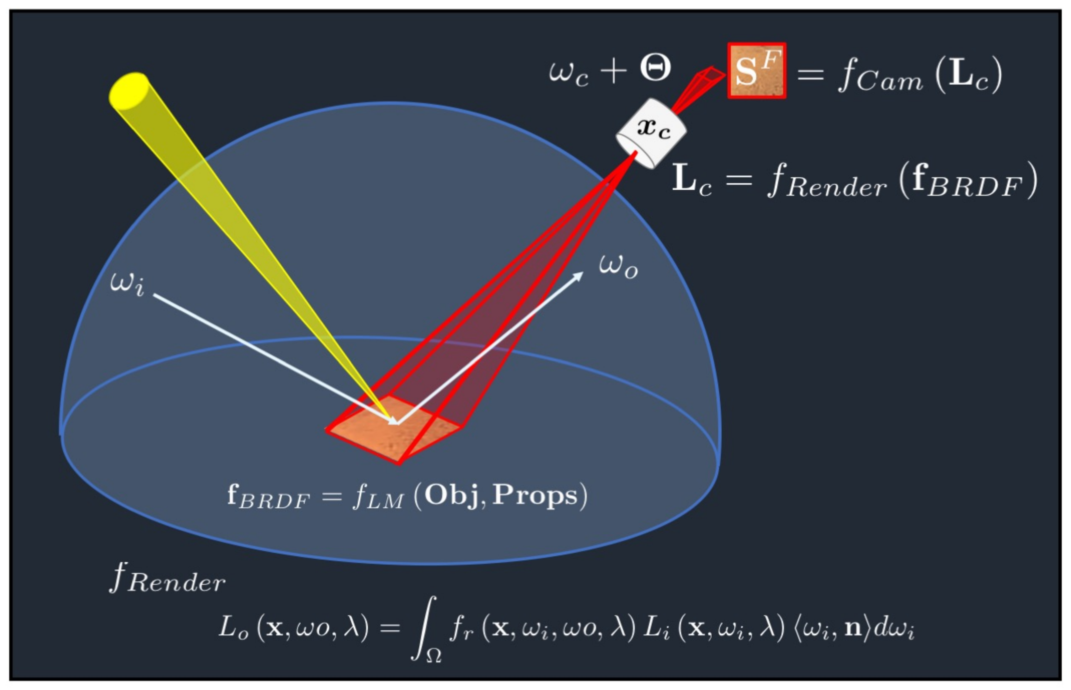

Figure 3: The geometry and notation of the *image chain*, including the form of the rendering equation.

In this work we formulate the function f_{Cam} for the specific case of the WACs, and present results and applications of a complete software simulation of the cameras.

The Camera Transfer Function

$$f_{Cam} : \mathbf{L}_c(\boldsymbol{x}_c, \hat{\omega}_c + \boldsymbol{\Theta}, \lambda) \rightarrow \mathbf{S}^F(\boldsymbol{x}_c, \hat{\omega}_c)$$

The camera forms a digital image from the inward spectral radiance at the point $\boldsymbol{x}_c$, the centre of the lens, with each pixel representing a direction in $\boldsymbol{\Theta}$, the field-of-view around the camera pointing direction, ω_c. f_{Cam} is composed of the functions outlined below:

$$Radiance \xrightarrow{Optics} Irradiance \xrightarrow{Detector} Image$$

Optics Function: from Scene Radiance to Focal Plane Irradiance

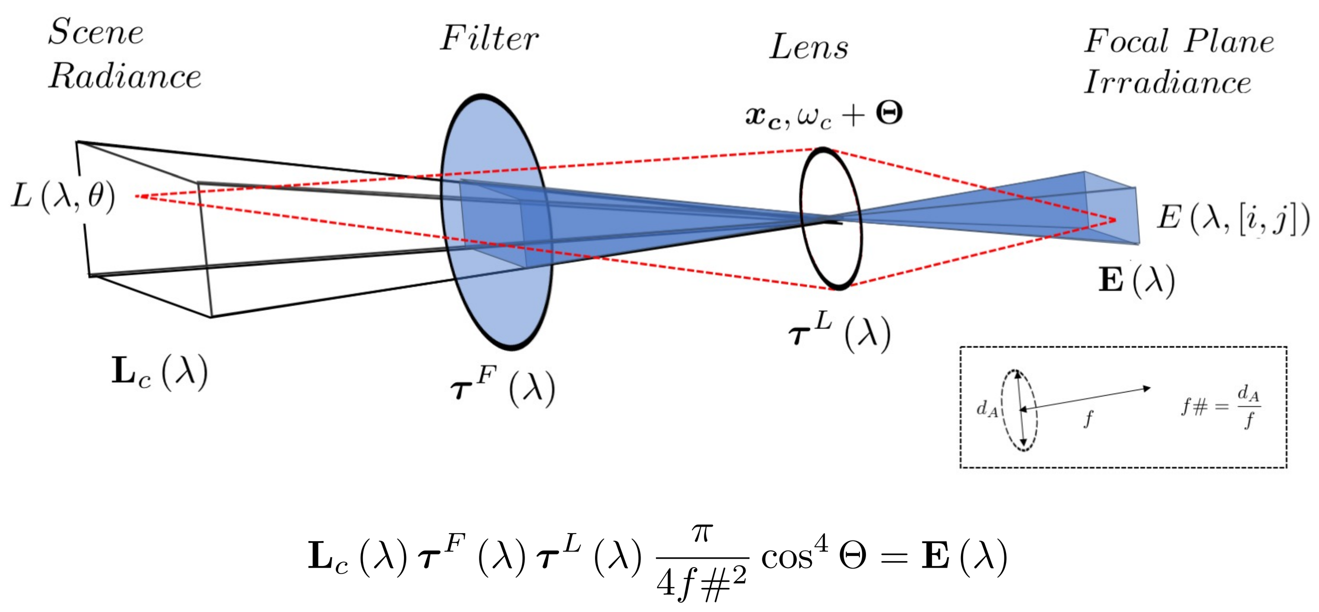

$$\mathbf{L}_c(\lambda)\,\boldsymbol{\tau}^F(\lambda)\,\boldsymbol{\tau}^L(\lambda)\,\frac{\pi}{4f\#^2}\cos^4\Theta = \mathbf{E}(\lambda)$$

Figure 4: The geometry and notation of the optics model. The spectral transmission in this model is directionally dependent, due to the wide (>15°) FoV of the WACs. The optics of previous multispectral cameras of surface missions have used FoVs <20°, and so could be described sufficiently by a single spectral transmission function for all directions.[4]

Detector Module: from Focal Plane Irradiance to Digital Image

$$Irradiance \xrightarrow{Pixel} Electrons \xrightarrow{SenseNode} Voltage \xrightarrow{FPGA} Voltage \xrightarrow{ADC} DN$$

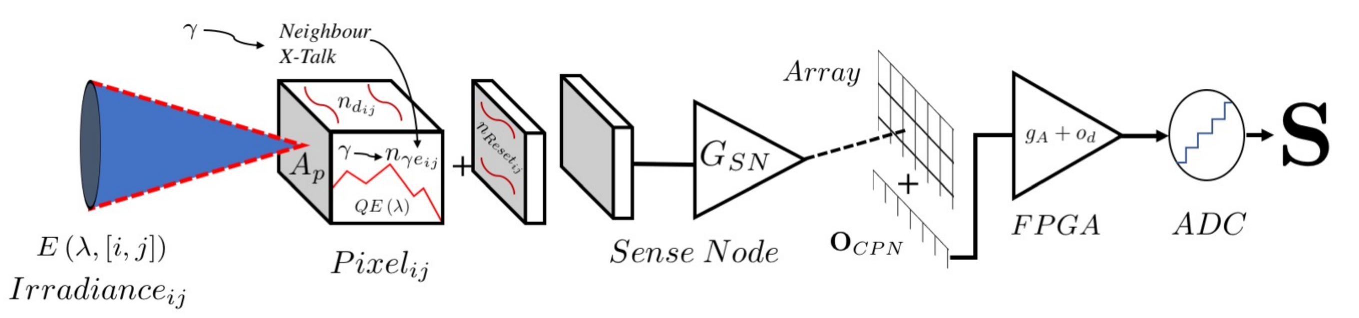

Irradiance to Electron Count

$$\mathbf{N}_{\gamma e} * \left[\begin{smallmatrix} xy & y & xy \\ x & 1-\Sigma & x \\ xy & y & xy \end{smallmatrix}\right] + \mathbf{N}_D + \mathbf{N}_{Reset} = \mathbf{N}_e$$

Photon Signal — *Thermal Noise*

Photo-electrons

$$n_{\gamma e_{ij}} \sim \mathcal{P}\left(q_{PR_{ij}} \frac{A_p}{hc} t_{exp} \int_\Lambda E_{ij}(\lambda)\,QE(\lambda)\,\lambda d\lambda\right)$$

$$q_{PR_{ij}} \sim \mathcal{N}(1, \sigma^2_{PRNU})$$

Dark-electrons[5]

$$n_{d_{ij}} \sim \mathcal{P}(t_{exp}\phi(T))$$

$$\phi(T) \sim \mathcal{LN}(\phi_\mu(T), \sigma^2_{DSNU})$$

$$\phi_\mu(T) = \phi_o 2^{\frac{T-T_o}{T_d}}$$

Reset Electrons

$$n_{Reset_{ij}} \sim \mathcal{N}\left(0, \frac{\sigma^2_{kT_o C} T}{T_o}\right)$$

Figure 5◀: Schematic and equations of the CMOS detector model, showing the pdf types used for each noise source. The parameters are chosen for accessibility from the Star 1000 detector datasheet[6].

Figure 6▶: We have formulated a new sense-node function, G_{SN}, giving an improved fit to electro-optical measurements, from the Star 1000 Datasheet, compared here against Gamma and Log best fits.

Electron Count to Digital Number

$$\left((G_{SN}(\mathbf{N}_e) + \mathbf{O}_{CPN})g_A + o_d\right)\frac{2^b - 1}{V_h - V_l} = \mathbf{S}$$

Amplification — *Quantisation*

Nonlinear conversion gain model

$$G_{SN}(\mathbf{N}_e) = \frac{V_{Sat} - a}{1 + \exp(bG_{Lin}(n_{FW} - \mathbf{N}_e))} + G_{Lin}\mathbf{N}_e$$

Column Amplifier Offset Noise

$$\mathbf{O}_{CPN} : o_{ij} = cpn_i \;\forall\, j$$

$$cpn_i \sim \mathcal{N}(1, \sigma^2_{CPN})$$

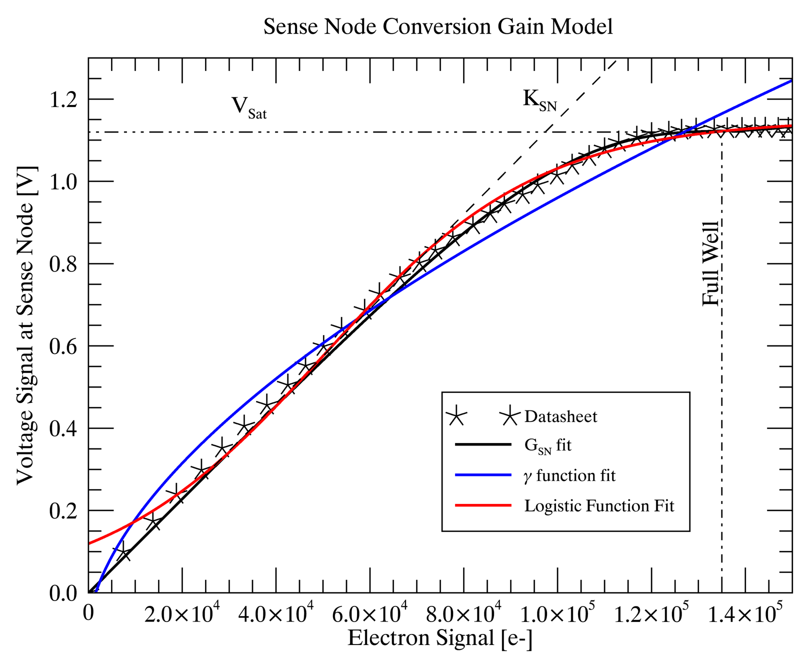

Features of the PanCam WAC Simulation

Language
IDL Object Oriented

Resolution
Spatial : 1024×1024 *(FoV Only – no stray light)*
Spectral : 701 channels, 400 - 1100nm, 1nm $\Delta\lambda$
Values : Double-precision

Data Inputs
Scene Radiance Cube *(W/m²/sr/µm)*
Filter Transmission Cube *(%)*
Lens Transmission Cube *(%)*
Quantum Eff. Vector *(e-/γ)*
Optics Vector *(4 misc parameters)*
Detector Vector *(30 misc parameters)*

@rbstabbins

Reconstructing spectral transmission for all angles

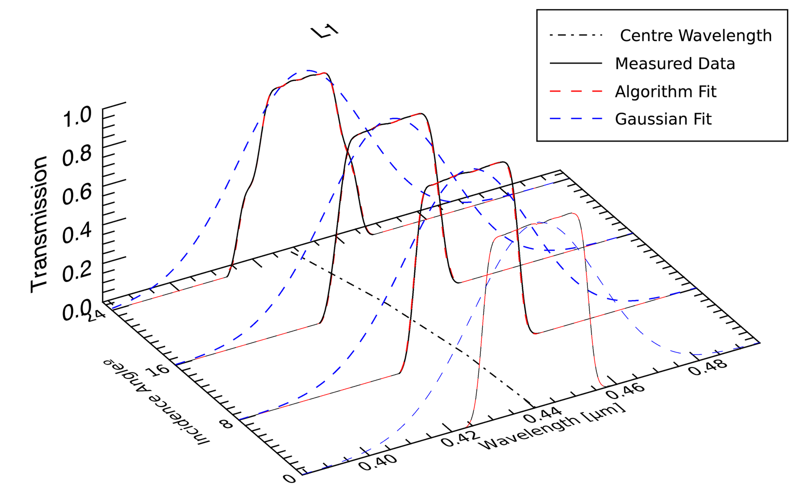

Figure 7: L1 example reconstruction, showing improvement on Gaussian fitting, by preserving changes in FWHM with θ, and maintaining the high kurtosis form of $\tau(\lambda)$. This has been repeated for all filters.

$\boldsymbol{\tau}(\lambda)$ is represented by a 1024x1024x701 cube. We have measurements of $\tau(\theta, \lambda)$ for $\theta_m \in \{0°, 4°, \ldots, 40°\}$ for each filter (from Aberystwyth University). We reconstruct the dense cube from sparse measurements by:

1. From $\tau(\theta_m, \lambda)$, find features $\lambda^{Centre}, \lambda^{FWHM+}, \lambda^{FWHM-}$ for each θ_m
2. Find n_{eff} by fitting the function $\lambda^f(\theta)$ to each feature.[7]

$$\lambda^f(\theta) = \lambda^f_o \cos\left(\sin^{-1}\left(\frac{\sin\theta}{n_{eff}}\right)\right)$$

3. For each measured $\lambda_i(\theta = 0°)$:
   i. Compute $\lambda_i(\theta_m)$
   ii. Fit a cubic polynomial to $\tau(\theta_m, \lambda_i(\theta_m))$
   iii. Interpolate $\tau(\theta, \lambda_i(\theta))$ for $\theta \in \{0°, 0.05°, \ldots, 26°\}$
4. This gives a dense function $\tau(\theta, \lambda)$, from which we can linearly interpolate $\boldsymbol{\tau}(\lambda)$ for $\theta_{ij} \in \Theta$

Preliminary Simulation Verification

Prior to the delivery of the PanCam flight model, the simulation serves as a prediction tool for camera performance. However, we still need to verify the workings of the simulation. We make preliminary verifications by simulating the scene radiance of a camera calibration environment, and compare results to calibration performed by the HRC team *(DLR)* on 5 Star 1000 RGB units.

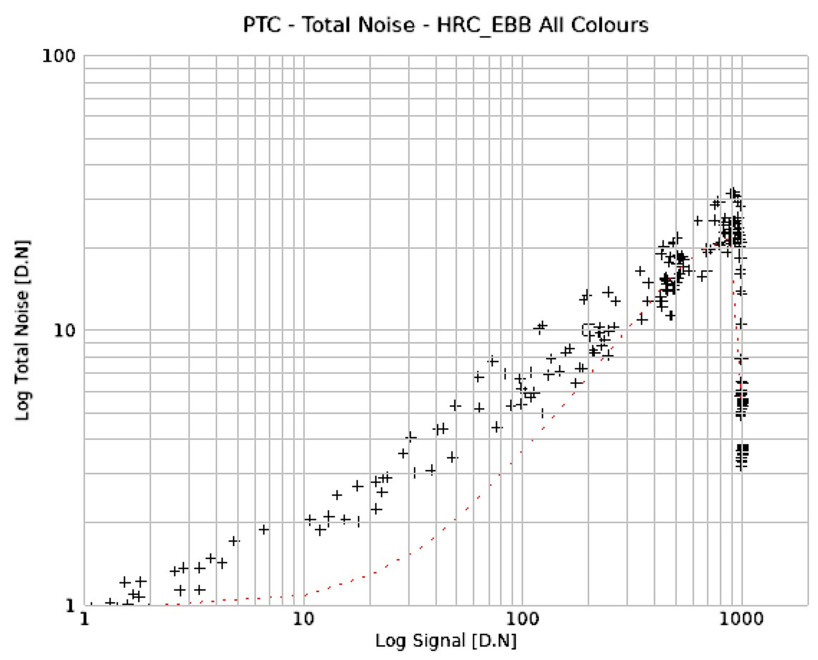

Figure 8: Photon Transfer Curve of Simulated (red) and 5x Star 1000 units (cross).

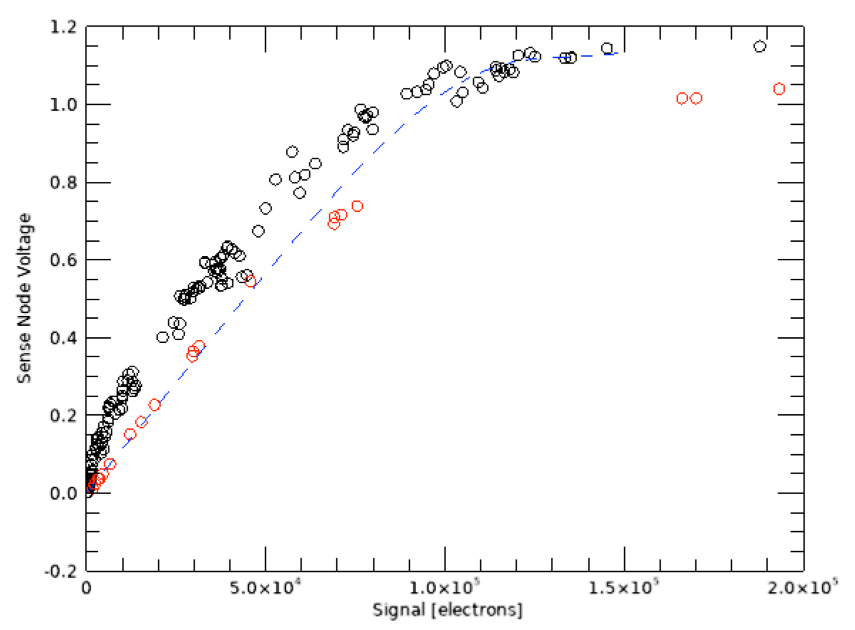

Figure 9: Simulated G_{SN} (blue) vs retrieved (red), and retrieved Star 1000 G_{SN} (black)

Use Case: Exposure Predictions for a generic synthetic scene

For a given scene radiance, there is an optimal exposure time. This is also dependent on the filter bandpass used, and the spectral power of the radiance for the filter wavelength. Longer exposures increase noise content, and so exposure predictions can inform us of the expected SNR for a particular filter.

Illumination
Sun : Zenith
Mid-Summer, Equator
Sky : SPD from Bell+ 2006[8]
OD 0.93, Airmass 1

Ground
Refl. Spec from Bell+ 2007[9]
Bright Soil (bl, bc)
Dark Rock (br)
White Rock (cl)
Bright Dune (cc)
Dark Rock (cr)

Calibration Target
Refl. Spec from Aber U.
Size simulated by Aber U.

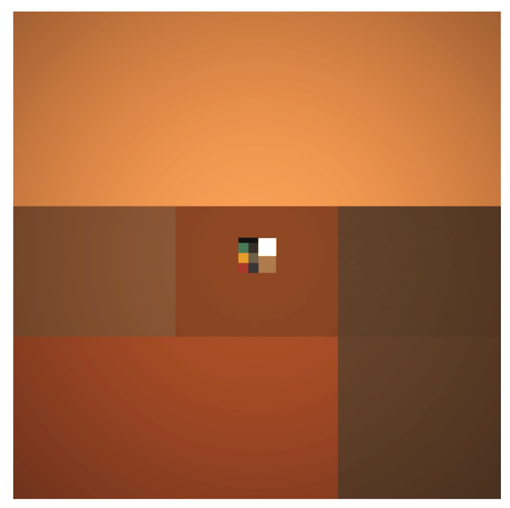

Figure 10: RGB sections from the hyperspectral cube of an abstract composition of soil and rock classes (identified by MER Pancam[9]), sky, and the PanCam Calibration Target.

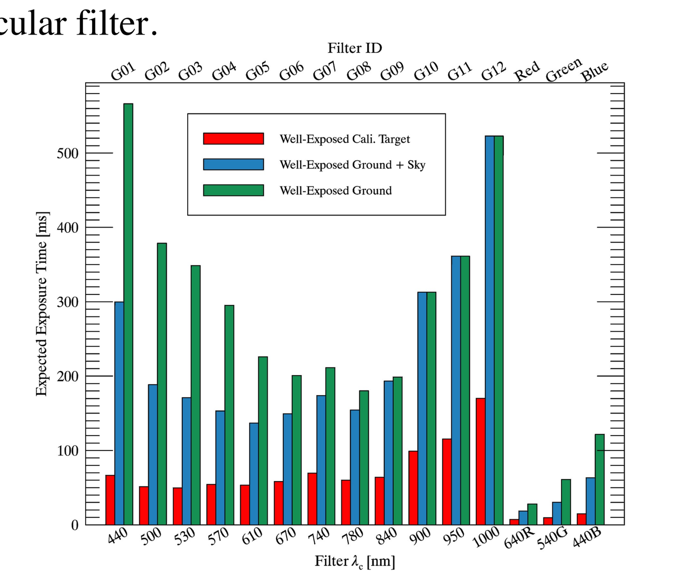

Figure 11: For each target, we can make predictions of the optimal exposure time for each filter channel.

Summary

- A forward model informs choice of inverse methods
- We present a Forward Model of the image capture of the PanCam WACs, featuring:
  - Directionally dependent transmission
  - Nonlinear CMOS Gain

Future Work

- Verification against PanCam FM/EM
- Rapid analysis tuning of inverse methods
- Merger with PBRT implementation of f_{Render}
- Library assembly of f_{BRDF} by experiment and collation

Institutions
[1]Mullard Space Science Laboratory, UCL, UK
[2]Centre for Planetary Science at UCL & Birkbeck, UK
[3]Department of Physics, Aberystwyth University, UK
[4]Institute for Planetary Research, DLR, DE

Acknowledgements
This research is funded by a UK Space Agency Aurora Studentship

Notation: **A** is a matrix of elements $a_{i,j}$ giving the value a for each pixel (i,j). $\mathcal{P}, \mathcal{N}, \mathcal{LN}$ give Poisson, Normal and Log-Normal deviates.

References
[1] Coates A. J. et al (2017) Astrobiology, [2] Vago J. L. et al (2017) Astrobiology, [3] Schott, J. (2007) Remote Sensing: The Image Chain Approach, Cousins C. R. et al (2012) Plan. & Space Sci., [4] Gunn M. & Cousins C. R. (2016) Earth & Space Sci., [5] Gow R. D. et al (2007) IEEE Trans. Elec. Dev., [6] On-Semiconductor (2015) NOIS1SM1000 A/D Star 1000 datasheet. [7] Macleod, H. A. (1989) Thin Film Optical Filters, [8] Bell, J. F (2006) JGR, [9] Bell, J. F (2007) The Martian Surface